Dear Editors,

Please consider our revised manuscript of “A spectral nudging method for the ACCESS1.3 atmospheric model” for publication.

We thank the reviewers for taking the time to review our manuscript and for their valuable feedback. We have taken each comment into account and believe the revised manuscript is much improved with these modifications.

In addition to the reviewer comments, we have made a few minor corrections to the manuscript. One change to note is that originally Figs. 1, 2 and 3, panels (c) and (d) had results from the simulations with filter length scales of lambda=0.03 and lambda=0.1 respectively rather than the 0.1 and 0.2 quoted in the caption. These figures have been updated to correctly use lambda=0.1 and lambda=0.2. This change does not affect any of analysis or conclusions in the paper. We apologise for this oversight in the original manuscript.

Another note is that Peter has added his affiliation with the Environmental Change Institute at the University of Oxford, and changed his correspondence email. Please let us know if that causes any problems.

Please see below our response to each of the reviewer comments. Note that page and line numbers refer to the manuscript rather than the document with tracked changes.

Best Regards,
Peter and Marcus

Response to Anonymous Reviewer #1:

General comments:

This paper describes a new spectral nudging scheme that has been implemented in the ACCESS climate model in order to constrain the model toward ERA-Interim (ERAI) reanalysis. The spectral nudging approach applies a low-pass spectral filter so that only large spatial scales are constrained. This filtering approach offers flexibility compared to Newtonian relaxation methods by allowing for the selection of the length scales as well as temporal scales to nudge. Since it is computationally expensive, the authors test implementations of 1-D filters compared to 2-D filters, as well as reducing the frequency that nudging is applied. Their analysis compares 500 hPa temperature between ERAI and several simulations including control (not nudged), Newtonian relaxation nudging, and 1-D and 2-D spectral nudging with several length scales. Based on their analysis, they conclude that using 1-D filters applied first in the meridional then zonal direction, and nudged once per hour, is the optimal, computationally efficient configuration.

The topic of the paper is a good fit for the scope of the journal. The description of the methods and results are clear. And the experiment design, testing several length scales and soft vs. hard nudging, is appealing. However, the analysis is very limited and only evaluates the impact of nudging on one model field (500 hPa temperature). Major revisions, providing much more detailed evaluation of the impact of this nudging approach on the simulated results, would be a greater benefit to the scientific community.

Observationally constraining a climate model, as is done here, implies a balance between (a) keeping the model state close to that of the host (ERAI) and (b) allowing the model to behave as it would in a “free-running” mode. The balance between (a) and (b) depends on the application. For example, Zhang et al. [2014] evaluate the use of nudging for aerosol-climate studies and find an undesirable impact of nudging on cloud and precipitation processes when strong temperature nudging is included, therefore suggesting only nudging horizontal winds for these types of studies. Jeuken et al. [1996] discusses in detail the implications for what variables are nudged and what relaxation times are used, identifying important considerations including: (1) how well the nudged fields (e.g. T, U, and V) match the reanalysis, (2) the magnitude of nudging tendencies (model forc-

ing) compared to model physics tendencies, and (3) the impact of nudging on unconstrained model fields (e.g. humidity, cloud water content, precipitation, etc.).

In this study only (1), how well the model is constrained, is evaluated, and only for 500 hPa temperature. For any application of this approach, it would be helpful to understand its impact on (2) model tendencies and (3) unconstrained model fields. The flexibility to nudge only large-scale features likely has benefits for reducing impacts on model behavior that can result from Newtonian relaxation methods, while still constraining circulation and meteorology. It is recommended that the analysis here be expanded beyond just evaluating 500 hPa temperature.

Response:

Although the original manuscript was focused on verifying that the scale-selective filter worked as designed, we acknowledge the reviewer's advice that the manuscript requires more evaluation so that the reader can better understand the implications of the technique. We have expanded our analyses to include T,U and V on 850, 500 and 250 hPa levels in section 3.1.1. This shows that U and V are also well constrained by the nudging and also depicts how errors over land become more pronounced as we approach the surface, due to differences between ERAI and ACCESS's land-surface parameterisation and topography. On the advice of the reviewer, we have also added a new section 3.1.2 with analysis of unconstrained variables, precipitation and mean sea level pressure. These fields were chosen as they are well constrained by observations. As suggested by the reviewer, we indeed find that the spectral filter has advantages with rainfall compared to the Newtonian relaxation.

Unfortunately, the particular version of ACCESS used for the experiments did not support output for model tendencies, although we have investigated the behaviour at diagnostic grid points. However, we feel that the comparison with the control (non-nudged) experiment provides similar information in-so-far as to where ERA-Interim and ACCESS disagree and therefore where the model tendencies would be the greatest (i.e., as for air temperature). We have added a sentence in section 3 (page 11 line 22) to clarify the use of the control simulation in reference to model tendencies, and we compare nudged simulations with the control simulation throughout the text.

We appreciate the reviewers comments on the design of the scale-selective filter and which fields to nudge. The Kanamaru and Kanamitsu reference that we mentioned also raises similar issues. We elected to stay consistent with the Telford approach and constrain Θ, U and V, which is a popular choice with many models. Although we agree that Newtonian relaxation can be detrimental for cloud and precipitation processes, we found that this issue was reduced for the spectral filter case and thank the reviewer for suggesting this analysis. This discussion is addressed in section 2.4 (from page 10 line 20) and we thank the reviewer for the additional references.

Specific comments:

1.
Page 6686 - line 17: A more detailed description of how ERAI was interpolated and prepared for the ACCESS grid would helpful. Vertical interpolation can create artifacts due to differences in model/reanalysis topography that can impact lower pressure levels high above the surface. Its possible the high temperature RMSE over mountain regions shown in Figure 1 is the result of topographic differences that were not properly accounted for in the interpolation scheme. How were ERAI and ACCESS topographic differences accounted for? What type of horizontal and vertical interpolation was used for temperature and winds? More description of the ERAI regridding procedure is needed.

The reviewer raises a valid point regarding the vertical interpolation method. For comparison with the original UM nudging paper by Telford et al, we elected to retain the same vertical interpolation that is based on a piece-wise linear interpolation based on the log of the pressure. No special treatment for orography was included for consistency with Telford et. al. Nevertheless, we have tried to highlight the problem in the revised text (page 10, line 10, page 20 line 8) and acknowledge that this issue needs to be addressed in future work. This additionally includes comments on other methods such as exploiting the lapse rate to correct air temperature, such as that used by the

Thatcher and McGregor reference. We have also added the information that ERAI data was interpolated to the ACESS horizontal grid using a bicubic interpolation method (page 10 line 5).

2.
Page 6687 - line 25: Figure 2 shows the "difference in variance of air temperature", but it is not discussed why this is a useful metric to evaluate or why the annual variance is too large in the control simulation and generally too small in the nudged simulations. A potentially more useful metric to quantify the degree to which ACCESS is constrained to ERAI would instead be the "variance of the difference in air temperature", which would show how nudging constrains the model to vary in the same way as ERAI, rather than just the amount of annual variability. Otherwise, more discussion is needed to clarify and explain the results shown in Figure 2.

Our aim in the original manuscript was to highlight the impact of nudging on the variance of fields as well as the mean behavior. We have analysed the variance of the difference, but we found that the errors were similar in spatial patterns and magnitude as was shown for the RMSE plots in figure 2. For this reason we felt that the difference in variance plots showed that the non-nudged ACCESS model underestimated this behavior and was somewhat corrected by the nudging. We have attempted to clarify the purpose of looking at the difference of the variance in the in the revised manuscript (from page 13 line 19).

3.
Page 6689 - line 1: It could be useful to show the map of RMSE with 2D and 1D filters (as in Figure 1) to justify that not only global mean error is similar, but the spatial distribution as well.

For the purposes of the manuscript we thought that showing zonal averaged RMS differences in figure 3 was the clearest way to represent the differences in spatial distribution of the 1D filters as the output from the two versions of the 1D filter and the 2D filter can be quite similar when viewed as a map. After consideration of the reviewer's comment, we have decided that it is helpful to modify figure 3 (now figure 7) to show the zonally averaged RMSE relative to ERAI rather than relative to the 2D filter, and also include the RMSE of the 2D filter in this plot. This shows how similar the three methods are, apart from in the high latitudes. The text for section 3.2 was adjusted to reflect the modification of this plot (from page 16 line 15).

4.
Page 6689 - line 9: Figure 4 shows RMSE levels off after 4 days. Were these first few days included in the subsequent analysis (all other figures) or was there some spin up time before the analysis period? Spin up is usually needed, and these differences between the initial conditions and reanalysis should not be part of the nudging evaluation.

Although we attempted to keep the experimental design simple for the reader, we acknowledge that the spin-up issue may be of some concern. To address this point, we have regenerated the plots and recalculated other values after omitting the first 10 simulation days, which avoids any spin-up problem. The results are very similar to those shown in the original manuscript and do not affect any of the conclusions of the manuscript. The text in the manuscript has been modified to reflect the different period of analysis (page 12 line 1).

5.
Page 6690 - line 7: A figure simply showing the difference between ACCESS simulations and ERAI could be helpful for illustrating that spectral nudging errors are random (positive and negative) and Newtonian relaxation is systemically warmer. What is the reason for this difference in the structure of errors with different approaches? Is this a result that is expected with the different implementations of nudging?

We acknowledge the reviewers comments regarding the confusion on the issue of systematic vs random errors. In the text, we were attempting to illustrate a possible situation that would result in one simulation having lower RMSE but greater GAE or vice-versa. We don't believe that these errors are a systematic result of the nudging and have removed this sentence to avoid confusion. We

have also changed our statement around the GAE to make it clear that when we look at different variables and different levels, the GAE does not always respond in the same way. In addition to this, we have made the point that for the control simulation, the standard deviation of the time series of the GAE is 0.7 K (page 14 line 7). This shows that the fluctuation of the errors in the control climate is much greater than the magnitude of any of the mean GAE values shown, so the GAE biases in the nudging simulations may reflect the behaviour of the control climate.

6.
Page 6690: It would be helpful to add the control results to Table 1 and include RMSE and GAE for U and V as well.

Thank you for these suggestions. We have included the control simulation results. We have also expanded Table 1 to include 250, 500 and 850hPa levels. We have added additional tables 2 and 3 for the results of U and V respectively.

7.
Do RMSE and RMS (Figures 1 and 3) show a similar result for horizontal winds? What do the errors look like for other pressure levels higher and lower in the atmosphere?

As discussed in the general comments, we are happy to address the reviewers comments with the inclusion of T, U and V errors for 250, 500 and 850 hPa levels. We have now included maps of RMSE for T at 250, 500 and 850 hPa in figures 1,2 and 3 respectively. The plots show an increasing difference between ACCESS and ERAI closer to the surface, likely to be arising from differences in the representation of land-surface processes and the topography, as well as because the bottom most levels are not nudged. We have produced similar maps for U and V, however decided that adding these did not add significantly to the manuscript compared to just showing the maps for T. The comparison between simulations for U and V is instead summarised in tables 2 and 3. These results are analysed in section 3.1.1 (from page 13 line 7).

8.
What is the magnitude of the nudging tendencies compared to model physics and dynamics tendencies? How much influence do model physics have on the simulation when nudging is applied?

As mentioned in the general comments, we acknowledge the reviewers interest in showing the model tendencies. Although this information was not available in the output of ACCESS in the version of the model we used, we instead tried to convey similar information from the comparison with the control experiment. For example, there is a temperature bias in the control run that the nudging tendencies will need to correct. Since the magnitude of this temperature error is reduced significantly by the nudging for 250 and 500 hPa levels, the nudging tendencies need to be significant compared to the tendencies arising from the rest of the simulation. For temperature at 850 hPa where the nudging doesn't have as strong an influence, is is clear that the model tendencies are dominating.

It was our intention to try to keep the analysis based on fields that are reasonable well constrained by observations and use the control experiment to explain where the nudging is making significant changes to the non-nudged model evolution. We have added a sentence in section 3 (page 11 line 22) to clarify the use of the control simulation in reference to model tendencies, and we compare nudged simulations with the control simulation throughout the text. We hope this addresses the reviewer's concern.

9.
How does the implementation of nudging impact convection, clouds, precipitation, surface fluxes, TOA radiation, etc.?

We thank the reviewer for their advice on analyzing the unconstrained fields. This is an effective test of how the non-nudged components of the model respond to the nudged fields. We prefer to concentrate our analysis on fields that are well constrained by observations and that are relatively easy to compare between models. So to that end we have concentrated our additional analysis on precipitation and mean sea-level pressure, which somewhat reflect the implications for convection, etc. The results for precipitation suggest that the scale-selective filter may have an advantage over the Newtonian relaxation in that case. This is addressed in section 3.1.2 with additional figures 5 and 6 presenting maps of RMSE for mean sea-level pressure and precipitation respectively.

10.
Page 6690 - line 5: Should it be λ = 0.2 instead of 0.1?

Thank you for this question. We can see that our purpose for this sentence could be clarified, so we have replaced it with a more general statement in section 3.1.1 (page 14 line 17): “The GAE can also have the opposite trend to RMSE. An example of this is shown for T in Table 1, where the hard relaxation nudging simulation, has a smaller RMSE but a larger magnitude of GAE compared to the hard spectral nudging simulations.”

Response to Anonymous Reviewer #2

General Comments:

This paper describes the implementation of the spectral nudging method described in Thatcher McGregor (2009) to the ACCESS1.3 model (which uses the Met Office Unified Model vn7.3 as its atmospheric GCM). This development makes use of the code existing from the work by Telford et al (2008) which implemented a Newtonian relaxation nudging method at an earlier Unified Model version. ERA-Interim reanalysis is used to drive the model. The experimental design is sound, and the technique, which allows for variations in the length scale of the nudging, is desirable in a model such as the UM.
The paper is well written and has an appropriate number of references. The various methods of nudging (occasionally known as "specified dynamics") are also concisely explained and clear, and the reasoning for the use of a 1D filter to approximate a 2D filter is sound. However, the use of 500hPa air temperature as the only evaluation variable is not sufficient and the results section should be greatly expanded to present results from a number of variables. It is important that the variables include those which are directly affected by the nudging, and others (such as mean sea-level pressure or precipitation) which are not.
Thatcher and McGregor presented analysis of 5 variables (surface pressure, mean sea-level pressure, zonal wind, meridional wind, and air temperature), mainly presented in tables or as a change in the variable with time. Telford et al examined 6 (potential temperature, zonal wind, vertical wind, surface pressure, precipitation, and specific humidity) presented these as a mixture of tables, column plots, lat/long plots, and zonal-mean plots.
The model set up here is similar to Telford et al, where a set year-long integrations are performed. In Telford et al data was presented for October, January, and July, rather than as annual means. Given the similarity between this study and Telford et al (in terms of the model set up) I am surprised that a more detailed analysis similar to that presented in Telford et al was not performed.
Major revisions to the analysis section are required before this paper is suitable for publication in GMD.

Response:

We thank the reviewer for their comments on the manuscript. Although our original aim was to focus on analysis that depicted the correct functioning of the spectral filter, we acknowledge that the manuscript could be improved by extending the analysis to other fields and other levels. We have expanded our analyses to include T, U and V on 850, 500 and 250 hPa levels in section 3.1.1. This shows that U and V are also well constrained by the nudging and also depicts how surface errors (i.e., over land) become more pronounced as we approach the surface due to differences between ERA-I and ACCESS's land-surface parameterisation and topography. On the advice of the reviewer, we have also added a new section 3.1.2 with analysis of the unconstrained variables, precipitation and mean sea-level pressure. These fields were chosen as they are well constrained by observations. This has been useful advice as the precipitation errors help to distinguish the scale-selective filter and Newtonian nudging methods. We have elected to continue with the annual analysis as it provides a slightly different perspective to the Telford et. al. work.

Specific comments:

1.
p 6682, line 10/p. 6686, line 20: while the behaviour of α is defined for the lower part of the atmosphere (near the boundary layer), what is not defined is how α is changed near the top of the atmosphere. The top panel from Figure 1 of Telford et al (nudging cut-off at level 50) would not apply here as ACCESS1.3 is in a 38-level configuration. Does the nudging occur all the way to the top of the model.

We thank the reviewer for pointing out that we have not properly explained the behavior of α in the upper atmosphere. We have indeed applied the nudging all the way to the top of the model, although ramping down the nudging over the last three levels. This information is now included in section 2.4 (page 11 line 6).

2.
p 6682, line 19: As the model description section does come until 2.4, it is unclear why the reanalysis resolution has been changed to 1.875◦ × 1.25◦ until we learn that.

The reviewer raises a valid point regarding confusion about the change in our reanalysis resolution compared to that used in Telford et. al. We chose this resolution to reflect the resolution of the ACCESS1.3 atmospheric grid. The statement about resolution of the ERAI reanalysis has now been moved from section 2.1 to the model description section (page 10 line 5) to avoid this confusion.

3.
p 6701, Figure 4: It is clear from this figure that there is a spin-up period of around 5-10 days or so. It is unclear if this spin-up period is also included in the other plots, which are all annual means. This could have an effect on these results. It would have been better to have performed a 13-month simulation and only used the final 12 months, or to take the approach of Telford et al and focus on specific months.

It was our original intention to keep the methodology simple in the original manuscript. However, we appreciate that the spin-up issue raises several questions regarding the results. To this end we have removed the first 10 days of the simulations from the analysis (with the exception of the monthly precipitation analysis), to avoid the spin-up issue. This is explained in section 3 (page 12 line 1). We have not seen any significant change in the results or for the conclusions of the paper.

We think this addresses the reviewer's concern, without complicating the description of the experimental design.

4.
p 6691, section 3.4 (Nudging period): I would suggest that this section should come before the preceding results sections, as it explains why the choice of 1-hour ("hard nudging") has been used throughout this paper (whereas e.g. Telford et al used 6-hour "soft nudging").

Thank you for making this point. We would like to clarify that section 3.4 explains the choice of 1 hourly application of the nudging correction (nudging period) as opposed to the 1 hour e-folding time ("hard nudging"). We will address the point of why we chose hard nudging as a separate issue to the order of the sections.

With regards to the order of the sections, there are a number of parameters that need to be explained and we decided that it suited the purpose of our paper to justify the use of the spectral filter before the nudging period. To make make the choice of parameters clear earlier in the manuscript, in section 2.4 (page 11 line 11) and section 3.3 (page 17 line 6) we refer to section 3.4 as to why we use spectral nudging applied once an hour rather than every time-step (as per Telford et. al.).

With regards to the 1-hour e-folding time "hard nudging", this was used in the majority of simulations in this paper although we did also present some results using the "soft nudging" as used by Telford et. al. The hard nudging was used as it is more consistent with our chosen configuration of the scale-selective filter. Essentially we did not want to unfairly disadvantage the Newtonian relaxation nudging, so compared the hard spectral nudging with the hard relaxation nudging. Nevertheless, we acknowledge that this point should have been made more clearly in the manuscript. We now note this point in section 2.4 paragraph 8.

Technical Corrections:
p. 6680, line 8: This should probably be "University of Cambridge, U.K."

Thanks for this advice. We have made this correction for the University of Cambridge in the revised manuscript (page 4 line 6).

Manuscript prepared for Geosci. Model Dev. Discuss.
with version 2014/07/29 7.12 Copernicus papers of the LaTeX class copernicus.cls.
Date: 5 May 2015

A spectral nudging method for the ACCESS1.3 atmospheric model

P. Uhe[1,2] **and M. Thatcher**[1]

[1]CSIRO Oceans and Atmosphere Flagship, 107–121 Station St, Aspendale, VIC 3195, Australia
[2]Environmental Change Institute, University of Oxford, Oxford, United Kingdom

Correspondence to: P. Uhe (peter.uhe@ouce.ox.ac.uk)

Abstract

A convolution based method of spectral nudging of atmospheric fields is developed in the Australian Community Climate and Earth Systems Simulator (ACCESS) version 1.3 which uses the UK Met Office Unified Model version 7.3 as its atmospheric component. The use of convolutions allow flexibility in application to different atmospheric grids. An approximation using one-dimensional convolutions is applied, improving the time taken by the nudging scheme by 10 to 30 times compared with a version using a two-dimensional convolution, without measurably degrading its performance. Care needs to be taken in the order of the convolutions and the frequency of nudging to obtain the best outcome. The spectral nudging scheme is benchmarked against a Newtonian relaxation method, nudging winds and air temperature towards ERA-Interim reanalyses. We find that the convolution approach can produce results that are competitive with Newtonian relaxation in both the effectiveness and efficiency of the scheme, while giving the added flexibility of choosing which length scales to nudge.

1 Introduction

Atmospheric modeling is a discipline that has impacts in many fields of scientific study as well as everyday life. For example, numerical weather prediction (Davies et al., 2005; Puri et al., 2013) provides us our daily weather forecasts and simulations of global climate (Taylor et al., 2012) give us forewarning of possible impacts of climate change. Global climate models are powerful tools, but they have limitations due to grid resolution, approximations to atmospheric physical processes (e.g., convection and turbulent mixing), and also because of incomplete or imperfect datasets such as for representing land-use. Furthermore, since the atmosphere is a chaotic system, the simulated synoptic patterns deviate from observations over time. This makes it more difficult to evaluate modeled behavior, since the advection of tracers depends on the synoptic scale atmospheric circulation. In some cases, to reduce biases caused by these issues, it is useful to introduce a correction to align the

model more closely with a host model, often an observational product such as the ERA-Interim reanalysis (ERAI; Dee et al., 2011). The process of adjusting dynamical variables of a model towards a host model is commonly known as nudging (Kida et al., 1991; Telford et al., 2008).

Nudging is useful for model development and scientific studies, where a more realistic atmospheric circulation can help determine errors or feedbacks in particular components of the model. Nudging in atmospheric models has been used to reduce the size of transport errors of trace gases for atmospheric chemistry (Telford et al., 2008) and carbon cycle modeling (Koffi et al., 2012), dynamically downscaling to finer resolution (Wang et al., 2004), and generating regional analyses (von Storch et al., 2000). Two popular approaches to nudging in atmospheric models are Newtonian relaxation (Telford et al., 2008) and spectral nudging (Waldron et al., 1996).

This paper describes an efficient method for implementing a convolution based spectral nudging scheme in atmospheric models, which is demonstrated using the Australian Community Climate and Earth System Simulator (ACCESS; Bi et al., 2013; Dix et al., 2013). The spectral nudging scheme can support irregular grids, making the approach applicable to a wide range of other atmospheric models. We have also significantly improved its computational efficiency by approximating the spectral nudging using one-dimensional (1-D) convolutions, and show that this does not degrade the performance. A convolution approach for spectral nudging using a cubic grid has previously been described by Thatcher and McGregor (2009). However this paper differs from the previous work, as the scheme in ACCESS has been designed to exploit the symmetries of the ACCESS latitude-longitude grid. This paper also provides an extended analysis to compare the performance of various configurations of nudging using Newtonian relaxation and spectral nudging.

ACCESS is a numerical model designed to simulate the Earth's weather and climate systems. ACCESS is used for a wide range of applications from climate change scenarios and numerical weather prediction, to targeted scientific studies into areas such as atmospheric chemistry and aerosols, and the carbon cycle. ACCESS is composed of a number of different submodels, of which the atmospheric component is the UK Met Office Unified

Model (UM; Davies et al., 2005; The HadGEM2 Development Team, 2011). The version of ACCESS used in this study, ACCESS1.3, includes the Community Atmosphere Biosphere Land Exchange model (CABLE; Kowalczyk et al., 2013) to represent the land surface. ACCESS often includes ocean and sea-ice components, but these components are not used in this study. A full description of ACCESS can be obtained from Bi et al. (2013).

Nudging was originally implemented in the UM at the University of Cambridge, UK (Telford et al., 2008), using a Newtonian relaxation method. This applies a correction to the model at every time step, calculated from the difference between the host model and the UM. The fields that are nudged are the key dynamical variables; Θ (potential temperature), U (zonal wind) and V (meridional wind).

An alternate approach to Newtonian relaxation is spectral nudging (von Storch et al., 2000; Thatcher and McGregor, 2009; Waldron et al., 1996). The spectral nudging scheme builds upon and expands the already existing Newtonian relaxation nudging code in the UM. It applies a low-pass spectral filter on the correction calculated as for the relaxation nudging, so the correction is only applied to large spatial scales. The spectral filter is applied using a convolution with a two-dimensional (2-D) Gaussian function. A convolution based filter was chosen rather than using a more conventional Discrete Fourier Transform, as it is simple to implement a parallel version within the UM framework and has the potential to be generalized to irregular and limited area grids. It also operates on the physical distance between grid points, which makes it straight forward to apply consistently across the whole globe and does not require special treatment of the poles. Spectral nudging gives the flexibility of being able to nudge the large scale features of the model towards the host, while allowing the small scales to be determined by the model's own physics. Because of this, spectral nudging is particularly useful in regional climate modeling (Denis et al., 2002; Kanamaru and Kanamitsu, 2007; Kida et al., 1991) and dynamical downscaling (Liu et al., 2012). In these cases, the model resolution is finer than the host model, so there is no information to nudge the finest length scales of the model towards, preventing the effective use of relaxation nudging.

The paper is structured as follows: Sect. 2 covers the implementation and configuration of nudging in ACCESS. This includes Sect. 2.1 covering relaxation nudging, then Sect. 2.2 describing the implementation of the spectral filter and the convolution method used to implement it. A 1-D filter that approximates the 2-D filter is described in Sect. 2.3. The 1-D filter gives significant improvements in the speed of calculating the filter and reduces the amount of message passing. The set up of the model used for simulations presented in this document is covered in Sect. 2.4.

The performance of the spectral nudging is analyzed in Sect. 3. This is split up into subsections relating to different indicators of its performance or looking at the behavior from different parameter choices. Section 3.1 compares ~~the nudged~~ nudged variables of the ACCESS model with ERAI, as well as the unconstrained fields of Mean Sea Level Pressure (MSLP) and precipitation. Section 3.2 compares the performance of the 1-D and 2-D spectral filters. Section 3.3 compares a number of different nudging configurations to see how closely they converge towards ERAI, and the effect of varying the spectral filter length scale. Lastly, Sect. 3.4 investigates the effect of varying the period of nudging, comparing its effect on the temporal spectrum and run times.

2 Nudging implementation

The process of nudging aims to perturb prognostic variables ψ_{m} of a model (e.g., ACCESS) toward the corresponding variable ψ_{h} of a host model (e.g., ERAI). The following section relates how nudging is implemented for each of the different methods used in this paper.

2.1 Newtonian relaxation

The standard Newtonian relaxation is applied by taking the difference between ψ_{m} and ψ_{h}, $\triangle\psi = \psi_{\mathsf{m}} - \psi_{\mathsf{h}}$, and using this to correct the model,

$$\psi_{\mathsf{m}} \rightarrow \psi_{\mathsf{m}} - \alpha\triangle\psi. \tag{1}$$

Here $\alpha \in [0,1]$ is a dimensionless constant determining the strength of nudging. α is related to the concept of an e folding time, which is the length of time to reduce the error by e^{-1}, where $\alpha < 1$. The e folding time is $\triangle t/\alpha$ where $\triangle t$ is the period of nudging. For example, a 6 h e folding time with nudging applied every half hour corresponds to $\alpha = 1/12$. α has vertical dependence, and is set to zero below 1000 m (i.e., the typical planetary boundary layer height). This helps avoid conflict between the nudging and the atmospheric model, since the behavior of the atmosphere in the boundary layer is strongly influenced by the land-surface, which can be different between the model and its host. α is also typically ramped down linearly from its full strength to zero over a several model levels to reduce the discontinuity between the nudged and non-nudged regions. It can also be ramped down at the top of the atmosphere to avoid any conflict that may occur due to top boundary conditions of the model.

The code used for the relaxation nudging is based on code from Telford et al. (2008) with some modifications. The code was restructured to improve parallelism when spatially interpolating host data and to use the ERAI dataset as the host model instead of other reanalysis products.

~~The ERAI dataset was also set up with horizontal resolution of 1.875east–west by 1.25north–south, compared to 3.75east–west by 2.5north–south in the reanalyses used by Telford et al. (2008) .~~

2.2 Spectral nudging

Spectral nudging extends the Newtonian relaxation method by taking the correction term and applying a spectral (low-pass) filter so that large spatial wavelengths are adjusted while smaller wavelengths are left essentially unperturbed. The method chosen to do this is based on Thatcher and McGregor (2009), using a convolution of $\triangle\psi$ with a Gaussian function, w, to implement the filter. However, the approach in this paper differs from previous work in its application to the ACCESS grid, requiring different implementation of the convolution for different underlying grids.

The correction for spectral nudging is applied as follows:

$$\psi_{\mathsf{m}} \rightarrow \psi_{\mathsf{m}} - \alpha(\triangle\psi * w) \tag{2}$$

where $*$ is the convolution operator. The convolution is calculated on the surface of a sphere (assumed to have radius $R = 1$). This results in:

$$\triangle\psi * w = \int\int \triangle\psi(\theta', \phi') w(\theta' - \theta, \phi' - \phi) \cos(\phi') \mathrm{d}\phi' \mathrm{d}\theta' \tag{3}$$

where the Gaussian weighting function is:

$$w(\theta' - \theta, \phi' - \phi) = \frac{1}{b} \exp\left(\frac{-\triangle\sigma^2}{2\lambda^2}\right). \tag{4}$$

λ is the standard deviation of the Gaussian function, which is referred to as the nudging length scale. θ and ϕ are the azimuthal angle and polar angle respectively, and θ' and ϕ' are dummy co-ordinates that are integrated over. b is a normalization factor, $b = \int\int \exp\left(\frac{-\triangle\sigma^2}{2\lambda^2}\right) \mathrm{d}\phi' \mathrm{d}\theta'$. Note that b is evaluated after the expression is discretized. $\triangle\sigma(\theta' - \theta, \phi' - \phi)$ is the distance of a chord between the two points (θ', ϕ') and (θ, ϕ):

$$\triangle\sigma = 2 \arcsin\left(\frac{C}{2}\right) \tag{5}$$

where $C(\theta' - \theta, \phi' - \phi)$ is the Cartesian distance between the points (θ', ϕ') and (θ, ϕ). Combining and discretizing Eqs. (3), (4) and (5), we get the correction that is applied by the scale selective filter.

The ACCESS grid is horizontally decomposed into domains that are assigned to individual processors. The calculation of the convolution at any point requires a global sum. Global information is not stored on individual processors, so the Message Passing Interface (MPI) is used to gather the $\triangle\psi$ arrays handled by each processor into a global array, and broadcast them to all processors. Each processor calculates the convolution just for its domain using this global information.

The naive implementation of the spectral filter involves a large computational effort (of order N^2 computations for N horizontal grid points). A spectral filter could be implemented more efficiently via a Fast Fourier Transform (FFT), or a spherical harmonic transform, requiring order $N \log_2 N$ computations, but the convolution gives much greater flexibility to be used with different grid configurations, from the regular latitude-longitude grid to irregular or limited area grids. To mitigate the computational effort of the convolution, a 1-D approximation to the convolution has been developed, described in the following section.

2.3 1-D filter

To improve the computational efficiency of the spectral nudging scheme, the 2-D convolution can be separated into two 1-D convolutions, thereby reducing the computational effort to order $N^{3/2}$. The 2-D convolution is separated by splitting the Gaussian function into parts that depend solely on latitude or longitude. The two integrals in the 2-D filter can then be evaluated separately as two 1-D convolutions. The expression for the two 1-D convolutions is equal to the 2-D convolution on a flat Cartesian grid, but is an approximation on a curved surface such as the global latitude-longitude grid.

$$w(\theta' - \theta, \phi' - \phi) \approx \frac{1}{b}\, w(\theta' - \theta, \phi) w(\theta', \phi' - \phi) \tag{6}$$

$$\approx \frac{1}{b} \exp\left(\frac{-\triangle\sigma(\theta' - \theta, \phi)^2}{2\lambda^2}\right) \exp\left(\frac{-\triangle\sigma(\theta', \phi' - \phi)^2}{2\lambda^2}\right). \tag{7}$$

A 1-D convolution is applied in one direction, then another 1-D convolution is applied on the result of the first convolution.

$$\triangle\psi * w \approx \frac{1}{b}[\triangle\psi * w(\theta', \phi' - \phi)] * w(\theta' - \theta, \phi) \tag{8}$$

$$\approx \frac{1}{b} \int \left[\int w(\theta', \phi' - \phi) \triangle\psi(\theta', \phi') \cos(\phi') \mathrm{d}\phi' \right] w(\theta' - \theta, \phi) \mathrm{d}\theta'. \tag{9}$$

Since the integrals are computed independently, w is calculated along horizontal rows and columns separately, not over the whole globe. Consequently, the code scales better with

increasing numbers of processors. As well as computational speedup, this reduces communication bottlenecks from data passed through MPI. Rather than global arrays being broadcast to every processor, each processor only needs data passed from processors associated with the same rows or columns of the horizontal grid.

Using this 1-D approximation, there is a choice in which convolution to apply first (i.e., either the zonal or meridional directions). Swapping the order of the integrals (convolutions) results in numerically different solutions. It is found that to reduce the error it is best to apply the convolution first along the latitudinal direction then longitudinally. This is discussed in Sect. 3.2, which compares the different orderings of the 1-D filter with the 2-D filter.

It also needs to be noted that the 1-D spectral filter is dependent on the model grid and the way the grid is decomposed into domains for each processor. The configuration of the ACCESS grid allows the convolution to be computed along rows of equal latitude or longitude and those results efficiently distributed to rows or columns of processors. This approach needs to be modified for grids which do not have these symmetries. See Thatcher and McGregor (2009) for an example of a 1-D spectral filter applied on a cubic grid.

2.4 Model configuration/description

This paper uses simulations of ACCESS, in the ACCESS1.3 atmosphere only configuration (Bi et al., 2013). This uses the atmospheric model UM vn7.3, CABLE 1.8 (Kowalczyk et al., 2013), as well as prescribed sea-surface temperatures and sea-ice concentrations. The model horizontally uses a N96 grid (uniform latitude longitude grid with 1.875° east-west and 1.25° north south resolution). It has 38 vertical levels which are terrain following hybrid height levels, representing heights from 10 m to 36 km. The model was run with a 30 min time step.

A series of one year simulations were run, starting from the 1 January 1990, each initialized in the same state, from a previous climate simulation, i.e. with an initial state unrelated to any historical synoptic patterns. The only differences between simulations were in the nudging configuration. These short experiments were chosen to to evaluate the performance of different nudging methods and choice of nudging parameters. Longer climate

simulations may also provide more in depth insight into biases in the nudging scheme, but this evaluation is beyond the scope of this paper.

The nudging component used the ERAI reanalysis product as the host model, provided at 6 hourly intervals. The ERAI data was ~~interpolated onto the ACCESS grid and~~ linearly interpolated temporally to each time step. It was interpolated horizontally using bi-cubic interpolation, from its native 0.75 east-west and 0.75 degrees north-south to a resolution of 1.875 degrees east-west by 1.25 degrees north-south, matching the grid used by the ACCESS1.3 atmosphere. This is a higher resolution than the ERA-40 reanalysis used in Telford et al. (2008) of 3.75 degrees east-west by 2.5 degrees north-south.

The ERAI dataset was interpolated vertically to the ACCESS1.3 model levels, using the vertical interpolation developed in Telford et al. (2008) , based on a piece-wise linear interpolation with respect to the natural logarithm of the air pressure. Some nudging methods include corrections to the vertical interpolation to account for the differences in orography between the simulation model and the host model (ACCESS1.3 and ERAI in this paper, respectively), such as exploiting the lapse rate to correct the interpolation of air temperature. However, since our goal in this manuscript is to evaluate the scale-selective filter compared to Newtonian relaxation, we have elected to retain the original interpolation scheme of Telford et al. (2008) for this study. Nevertheless, orographic adjustment for interpolated fields is an important topic that we intend to address in further work.

Nudging was applied ~~above~~ to potential temperature (Θ), zonal wind (U) and meridional wind (V). The choice of which prognostic variables to nudge is an important aspect of the experiment design. Kanamaru and Kanamitsu (2007) argued that the U, V wind components, temperature, water vapour and surface pressure all needed to be nudged to sufficiently constrain the large scale biases of the model. Jeuken et al. (1996) also highlighted the effect nudging can have on the model physics if the nudging terms become too large. For simplicity, we have chosen to nudge the Θ, U, and V so as to be consistent with the nudging approach used by Telford et al. (2008) . Note that we specifically avoid nudging the water vapour due to its potentially highly non-linear behaviour in the presence

of clouds. We specifically consider whether the nudging is unbalancing the model in section 3.4 in the context of the temperature temporal spectra.

The nudging adjustment was only applied from vertical level 7, corresponding to about 1 km in height above the surface terrain. The nudging amplitude α ~~,~~ was ramped up from 0 to the full strength over 3 vertical levels so as to reduce the discontinuity between nudged and non-nudged parts of the atmosphere. α was also ramped down over the top 3 vertical levels of the model.

The parameters varied in the experiments were the nudging method, nudging period, maximum nudging strength, and spectral filter length. The relaxation nudging is always applied every time step, and the spectral filter can be applied at frequencies that are multiples of the time step and divide into 6 h (e.g. 0.5, 1, 2, 3 or 6 h). Most spectral nudging simulations analysed in this manuscript have nudging applied at a frequency of 1 h, which is justified in Sect. 3.4.

Simulations presented use a maximum nudging strength corresponding to either a one hour e folding time (referred to as hard nudging) or six hour e folding time (referred to as soft nudging). We note that soft nudging is used in Telford et al. (2008) and is a common choice for relaxation nudging. In this paper we find it useful to compare soft relaxation nudging with the soft spectral nudging and hard relaxation nudging with hard spectral nudging. Simulations were run with a range of filter length scales, from 0.03–0.5 radians.

3 Results and discussion

To determine the performance of the spectral filter, we look at the nudged runs compared with ERAI, as well as comparing with a control simulation without nudging. The control simulation also gives an indication of the behaviour of the nudging tendencies that were required to change the evolution of the simulation. The analysis was conducted ~~in all cases on the air temperature field~~on the nudged air temperature and wind fields, measured on ~~a plane~~ planes of constant pressure at 250, 500 and 850 hPa. Note that although the potential temperature Θ is nudged, we actually evaluate the the air temperature T,

when comparing the simulated results with ERAI. Two unconstrained fields, MSLP and precipitation were also evaluated. Except where specified otherwise, the whole one year period of the simulation excluding the first 10 days was used. Excluding this period from the analysis ensures the atmosphere is settled fully into the nudged state.

After describing the impact of nudging in section 3.1, we compare different implementations of the 1-D and 2-D spectral filters in section 3.2 and then evaluate the influence of using different spectral filter parameters in section 3.3. Lastly section 3.4 gives a justification for the selection of the period of application of spectral nudging which is used throughout this manuscript.

3.1 Analysis of mean state and variance in the nudged model

~~Figure ??~~

3.1.1 Effect of nudging on nudged atmospheric fields

Figure 1 shows the spatial distribution of root mean squared error (RMSE) at 250 hPa for different ACCESS simulations, where we are defining the error as the difference between ACCESS and ERAI~~and calculating it~~. It is calculated over one year of simulation apart from the first 10 days, for the 6 hourly intervals the ERAI data is provided on. For these plots, a control simulation with no nudging is compared against simulations using relaxation nudging and spectral nudging. The different behaviour between the nudged and control simulations provides an indication of the strength of the nudging tendencies. The 1-D filter was chosen as the preferred method of spectral nudging as discussed further in Sect. 3.2. In all cases, the nudged runs have much smaller error than the control simulation, indicating closer agreement with ERAI. The spectral filter with small length scales nudged (Fig. ~~??~~1c) results in behavior similar to the relaxation nudging (Fig. ~~??~~1b). As the filter length scale is increased, larger wavelengths are able to deviate from ERAI, and the magnitudes of the deviations are larger (Fig. ~~??~~1d).

~~It is also worthwhile to note the greatest deviations occur over~~

Figures 2 and 3 show the same data as Fig. 1, except lower in the atmosphere, at levels of 500 hPa and 850 hPa respectively. As the height decreases, we notice differences in the simulation over high orographic features such as the Himalayas, Antarctica or the Andes. These differences become more pronounced with the 850 hPa results, which is close to the lowest atmospheric levels that are nudged. We would expect there to be some differences between ACCESS and ERAI near the surface due to different representation of land-surface processes and different boundary layer parametrizations between the different atmospheric models. However, the largest errors are located where there is ~~a mismatch in the~~ likely to be a mismatch in orographic height between ACCESS and ERAI and may suggest a limitation of the current method of interpolating ERAI to the ACCESS grid.

The U and V winds show similar trends in the relative RMSE between different simulations as those shown for temperature in Figs. 1, 2 and 3. This is demonstrated by the global average RMSE of these fields, shown in Tables 2 and 3. These tables present data at atmospheric levels of 250, 500 and 850 hPa. We note that all of the nudging simulations are more strongly constrained in RMSE than the control simulation with no nudging. This is true for each of the variables, at each level. At 850 hPa which is close to the lowest atmospheric levels that are nudged, the U and V winds have an average RMSE similar to the higher atmospheric levels. In contrast, the air temperature average RMSE shown in Fig. 1 is multiple times greater than the higher atmospheric levels. This shows that temperature is more affected by the surface and orographic differences. We also note that the hard nudging simulations are more constrained in RMSE than the equivalent simulations with soft nudging in all cases.

Since we intend to use the nudging in the simulation over climate timescales (i.e., decades), it is useful to determine how well the simulation predicts the variance as well as the mean air temperature. Figure 4 shows the ~~difference~~ differences in the variance of air temperature between the ACCESS simulations and ERAI ~~. The variance in the ACCESS control simulation is consistently higher than ERAI , shown in Fig. 4a. Nudging constrains the variance to much more closely match the variance in ERAI than the~~ at 500 hPa. Note that ACCESS consistently overestimates the variance of the air temperature in the con-

trol ~~simulation. There is a similar magnitude of difference in the variance for each of the~~ experiment compared to ERAI (Fig. 4a), presumably as a consequence of imperfect physical parametrizations. We note that this overestimate of the variance in air temperature is reduced by the nudging, with the difference in variance for Fig. 4b-d being an order of magnitude less than Fig 4a.

It is also useful to compare the performance of the model between small and large spatial scales. The RMSE gives the error grid point by grid point, at the smallest length scale. To evaluate the error at the largest length scale (the whole globe), the global mean of the difference between ACCESS and ERAI can be used. We refer to this as the Global Average Error (GAE). Values for the GAE are included in Tables 1, 2 and 3 for T, U and V respectively. This covers each of the atmospheric fields nudged in our simulations at different heights in the atmosphere. In addition to the values in the tables, we note that the GAE tends to fluctuate rather than settle down to a constant value. For example, the mean GAE of air temperature at 250 hPa for the control simulation is -0.37K but its standard deviation is 0.7K. The nudged simulations which have lower mean GAE, also have a corresponding lower standard deviation of GAE of 0.01–0.04K. This shows smaller fluctuations in the GAE of the nudged simulations and the control simulation.

Tables 1, 2 and 3 also show that the simulations that are more tightly constrained in RMSE do not necessarily result in lower GAE. This is very dependant on the variable and vertical level looked at. For example, looking at V at 500 hPa in Table 3, the hard nudging simulations which are more constrained in RMSE have a lower GAE than the control, whereas the soft nudging simulations are not noticeably improved relative to the control simulation. However for V at 250 hPa, the GAEs for all of the nudged simulations are reduced by an order of magnitude relative to the control simulation and there is very little difference between the nudged simulations. The GAE can also have the opposite trend to RMSE. An example of this is for T in Table 1, where the hard relaxation nudging has a smaller RMSE but a larger magnitude of GAE compared to the hard spectral nudging simulations. ~~The nudged simulations have greater variance than ERAI over some land masses, but lower variance over the oceans. Investigation into the reason for this is the subject of~~

~~future work.~~ ~~Hence~~ there is no nudging approach that clearly produces superior GAE results for all measures. However, the GAE for nudging simulations is comparable or lower than the control simulations for all cases, and there are only a few values that are not improved when nudging is introduced.

3.1.2 Effect of nudging on unconstrained atmospheric fields

In addition to constraining the nudged parameters, it is important that the nudging does not have a detrimental effect on other atmospheric processes. For this study, we examine the simulated MSLP and precipitation. We have chosen to concentrate on these fields since they can be readily compared to ERAI results and can also potentially be tested by observational data. For simplicity, in this paper we will compare the simulated results to ERAI predictions, noting that ERAI also produces an imperfect simulation of rainfall. A more detailed discussion of how nudging can effect model physics can be found in Jeuken et al. (1996) . The spatial distribution of the RMSE of MSLP and precipitation are shown in Figs. 5 and 6 respectively, for the different nudging methods discussed in this paper. The results show a reduction in the RMSE in the nudged simulations (Fig. 5b-d) compared to the control simulation (Fig. 5a), illustrating that the simulated MSLP is responding favourably to the nudging. Differences between the ACCESS simulated MSLP and ERAI are more noticeable for regions of high orography, although this may be attributable to differences in the method used to calculate MSLP under orography. The magnitude of the MSLP RMSE is similar for each of the nudged simulations, although MSLP is a relatively smooth field and can be less sensitive to smaller scale differences in the nudging.

In Fig. 6 we consider the RMSE of the monthly mean rainfall. To cover the whole seasonal cycle, the one year simulation including the first 10 days was used in this analysis. As the ERAI precipitation is calculated by a model with different physics to ACCESS1.3, differences in specific rainfall events are expected. Due to this and the significant spatial and temporal variability in rainfall, the monthly mean values were chosen to provide a more consistent interpretation of precipitation biases than comparing higher frequency data. This only

allows us to evaluate the spatial distribution of the rainfall rather than the timing of rainfall events. Each of the nudged simulation have improved the monthly precipitation compared to the control simulation. However, Fig. 6b, shows a worsening of the RMSE for the hard relaxation method over a few limited regions such as the Himalayas and Andes compared to the control simulation (Fig. 6a). This issue is also present in the soft relaxation nudging simulation (not shown) and this result is consistent with Zhang et al. (2014) , who found that Newtonian relaxation could have a detrimental effect on the cloud and precipitation processes due to temperature nudging. However, Fig. 6c and d, using spectral nudging, have reduced this issue or even removed the problem in some locations. It is clear that leaving smaller length scales unperturbed by the spectral filter is advantageous for the model physical parameterisations at least when simulating rainfall processes, even for the relatively strong nudging case shown in Fig. 6.

3.2 Evaluation of 1-D filter approximation

The ~~approximation used in~~ majority of results presented in this manuscript are for nudging simulations using the 1-D ~~spectral filter can be tested by comparing the results with simulations~~ filter. To justify this choice of spectral filter method, in this section we compare the results of different configurations of the 1-D filter to that obtained using the 2-D filter. There are two ways to order the convolutions in the 1-D filter, with the zonal convolution followed by the meridional convolution (1-D filter, lon-lat), or the meridional convolution followed by the zonal convolution (1-D filter, lat-lon).

The ~~global Root Mean Squared Error (RMSE)~~ RMSE of air temperature at 500 hPa is very similar between the different methods of spectral nudging. Simulations using hard nudging and a filter length of $\lambda = 0.1$ applied once an hour, give an RMSE of ~~0.415~~0.407 K for the 2-D filter ~~, 0.414K for~~ and the 1-D filter lat-lon~~and 0.416~~, compared to 0.408 K for the 1-D filter lon-lat, in air temperature at 500 hPa, over one year of simulation (excluding the first 10 days).

To more closely compare the different ordering of the 1-D convolutions, Fig. ~~?? shows the RMS difference between~~ 7 shows the zonally meaned RMSE of simulations using the 1-D

filters and the 2-D filter. In polar regions, there is a greater ~~difference between the~~ RMSE in the 1-D lon-lat case compared to the 2-D filter and the 1-D ~~filter in the lon-lat case,~~ lat-lon. This indicates that the lat-lon case is a better approximation of the 2-D filter than the lon-lat.

The difference between the lon-lat and the lat-lon version of the 1-D filter occurs because the grid points near the pole are physically close together in the longitudinal direction. A small error at the pole could be spread zonally across multiple grid points. In the lon-lat case, this error will remain after the initial zonal convolution. On the other hand, when the meridional convolution is applied first, the error near the poles can be reduced. This is because the values at grid boxes close to the poles have a smaller weighting in the meridional convolution as they have a smaller area.

~~The other differences between~~ As the 1-D ~~and 2-D filter shown in Fig. **??**, can be attributed to small numerical differences which grow over time in a chaotic system. These differences are especially noticeable near the equator. However, the time averaged RMSEs relative to ERAI quoted above, show no significant difference between the 1-D and 2-D filters. Hence the 1-D filter gives a different result to the 2-D filter, but~~ filter constrains the model to a ~~similar extent . Because of this, and the reduction in computational effort compared to the~~ similar extent as the 2-D filter, ~~the~~ with much reduced computational effort, it is clearly the preferred choice. The 1-D filter with the meridional convolution applied first ~~is taken as the optimum choice~~has better performance at the poles, so it is the optimum configuration. All simulations using spectral nudging refer to this configuration, except where specified otherwise.

3.3 Performance of the spectral filter

Figure 8 shows time-series of RMSE of air temperature at 500 hPa for relaxation and spectral nudging simulations, using different filter length scales and e folding times. Each spectral nudging simulation uses hourly nudging ~~.~~as discussed in Sect. 3.4. The convergence of RMSE depends on the combination of e folding time and nudging length scale (for the spectral nudging). The model is more tightly constrained using the shorter e folding time (hard nudging) and smaller nudging length scales. The spectral filter with $\lambda = 0.1$ and one

hour e folding time, gives a RMSE similar to the relaxation nudging with a six hour e folding time. The more tightly constrained simulations reach a steady state more quickly, and all the simulations shown have reached a steady RMSE within four days of simulation or less (not visible for the time scale of this plot).

~~It is also useful to compare the performance of the model between small and large spatial scales. The RMSE gives the error grid point by grid point, at the smallest length scale. To evaluate the error at the largest length scale (the whole globe), the global mean of the difference between ACCESS and ERAI can be used. We refer to this as the Global Average Error (GAE). The GAE tends to drift over time rather than settle down to a constant value, so the values of GAE presented in Table **??** include a 95~~Tables 1, 2 and 3 show the temporally and spatially averaged RMSE and GAE for each of the nudged fields T, U and V at 250, 500 and 850 ~~confidence interval as a measure of the uncertainty. Future work will involve conducting multi-year simulations to obtain more conclusive statistics regarding biases or trends in~~ hPa levels. The simulations shown in these tables have the same relationship in RMSE as shown in Fig. 8. In particular, for a given strength of nudging, the relaxation nudging has the smallest RMSE, the spectral nudging with $\lambda = 0.03$ is closest to the relaxation nudging, and the RMSE increases for the spectral nudging as the filter length increases. This is true for each of the ~~GAE~~variables T, U and V, at each level evaluated. In addition, the hard nudging simulations result in smaller RMSE than the equivalent set up using soft nudging.

~~Table **??** shows that the simulations that are more tightly constrained in RMSE do not necessarily result in lower GAE, though we do note that the more tightly constrained simulations have smaller fluctuations in~~ As seen in section 3.1.1, the ~~GAE (not shown). For example~~GAE is generally improved in comparison to the control simulation. In addition, the hard spectral nudging with ~~$\lambda = 0.1$ has a greater RMSE, but smaller GAE than the hard relaxation nudging . The RMSE quantifies how large the magnitude of errors are at each grid box whereas the GAE indicates how much ACCESS is warmer or cooler than ERAI, averaged over the globe. The smaller GAE for the spectral nudging can be explained by the relaxation nudgingresulting in smaller errors at each grid box, but a tendency for those~~

errors to be in the same direction (warmer), while the spectral nudging has larger errors at each grid box but with these errors averaging out at the large spatial scales. the smallest filter length, $\lambda = 0.03$ produces GAE that are reasonably consistent with the relaxation nudging results. However, when comparing the different nudging methods, there is no clear pattern across levels and variables. For hard nudging, the spectral filter simulations have a smaller temperature GAE at all levels compared to the relaxation nudging, but the same is not the case when looking at the soft nudging simulations or when evaluating U and V. Hence, there is no clear advantage of any particular nudging method when evaluating the model performance in terms of GAE.

To further show the effect of the spectral filter at different length scales, the simulation output was re-gridded to a range of coarser resolutions. Re-gridding to coarser resolutions removes the fine scale detail in a similar way to the spectral filter, so the performance of the spectral filter should improve at coarser resolutions. This is shown by Fig. 9, which compares the RMSE at different re-gridded resolutions for different simulations.

At the highest resolutions, the relaxation nudging has a smaller RMSE, showing that it constrains the small length scales more tightly than the spectral nudging. For the spectral nudging, decreasing λ reduces the RMSE at all length scales (i.e. shifts the curve downward). At coarser re-gridded resolutions, the spectral nudging simulations with $\lambda = 0.1$ and $\lambda = 0.2$ have lower RMSE than the relaxation nudging. Hence, the spectral nudging can capture the large scale structures of ERAI better than the relaxation nudging. The spectral nudging with $\lambda = 0.5$ has a greater RMSE for all re-gridded resolutions apart from the largest, indicating that the filter is not as effective at constraining the model in this case. From this we can choose relaxation nudging or spectral nudging with a smaller or greater λ, depending on which spatial length scales we want to constrain.

3.4 Nudging period

Figure 10 shows the temporal spectra of the 500 hPa air temperature from simulations using different nudging configurations. Relaxation nudging is applied every time step, so the

nudging period is only applicable to the spectral filter. Nudging can be applied at intervals from every time step (30 min), to the period of the host data (6 h in the case of ERAI).

All valid choices of nudging period are able to sufficiently constrain the model, given a comparable e folding time. The choice of nudging therefore, is a trade-off between computational effort and increased nudging shock, as constraining the model when nudging less frequently requires larger adjustments to the perturbed field. Nudging less frequently hence causes distortions to the temporal spectra as shown in Fig. 10. However less frequent nudging offers a significant speedup as discussed below.

Examining Fig. 10 in more detail, it is evident that nudging with a period of six hours results in spikes in the Fourier spectrum at certain frequencies. This shows that the nudging adjustment is unbalancing the atmospheric model, causing it to respond unevenly in the spectrum. When nudging every hour, these imbalances are removed. Apart from a distortion in the spectrum below half an hour (one time step), the line for spectral nudging every hour lies on top on the line for spectral nudging every time step.

The spectra when nudging every time step is qualitatively similar to the control simulation, but shifted down in magnitude. The spectral nudging every time step has a spectrum in between the curves for the control and relaxation nudging. The spectrum for the 2-D filter is indistinguishable to the equivalent simulations using the 1-D spectral filter with the same filter length scale (2-D filter not shown).

Considering the speed benefits of different nudging frequencies, the 1-D spectral filter nudged every 6 h adds 3.3 % to the run time (the same as Newtonian relaxation). When the period is decreased to 1 h or 30 min this increases the run time by 6.7 and 12 % respectively. The 2-D spectral filter in comparison adds 33 % when nudged every 6 h, increasing to 190 and 376 %, which is not viable for most uses.

Nudging at hourly intervals can be used as a compromise between speed of computation and reducing the distortions in the spectra, and is the standard period of nudging used for spectral nudging in this paper.

4 Conclusions

This paper has introduced the use of spectral nudging in the UM and ACCESS. This is achieved through a novel convolution method, first described by Thatcher and McGregor (2009), but generalized in this paper for use with latitude-longitude grids as used by the ACCESS atmospheric model. Analysis of the different configurations of nudging shows that the nudging schemes effectively constrain the nudged fields to follow the host model (ERAI). We have surveyed the spectral filter across a range of filter length scales. The spectral nudging scheme approaches the Newtonian relaxation nudging when small length scales are nudged, but allows the flexibility to nudge only large spatial structures when the filter length scale is increased.

Our results show that simulation errors in air temperature are greater near the surface for all nudging methods, which is expected due to the different representation of land-surface parametrizations. Although our objective was to compare the Newtonian relaxation with the spectral filter in ACCESS, we note that differences occur where there is a mismatch in the orographic height between the ACCESS simulation and ERAI, suggesting a problem with the vertical interpolation to the ACCESS grid used by the nudging. We intend to address this problem in future work.

We have also considered the implications of nudging on MSLP and precipitation which are not directly perturbed by the nudging. MSLP is a reasonably smoothly varying field and is well constrained by the nudging in all simulations to agree with ERA-Interim. There are some differences under high orography, although this may be more related to the method used for calculating MSLP under orography, rather than the nudging method. The nudged simulation improved the monthly mean rainfall compared to the control simulation. Furthermore, the spectral nudging simulations predicted rainfall that was in closer agreement with ERAI, than the relaxation nudging simulations. This provides an example of where the spectral filter can have an advantage over the Newtonian relaxation approach, particularly for physical processes that are sensitive to the local behaviour of the atmosphere.

The 1-D spectral filter is shown to perform as well as the 2-D filter, while producing a speedup of 10–30 times. This is achieved by the approximation of separating the 2-D convolution into 1-D convolutions and by using symmetries of the model grid to reduce communication between processors. We also identified that due to the geometry of our grid, the order of convolutions in the 1-D filter was important. To reduce error in the approximation, the meridional convolution is applied first.

Nudging with different frequencies was also investigated, showing that nudging every six hours is still able to constrain the model, but introduces distortions to the spectra. Nudging once an hour produces a speed up in comparison to nudging every time step, while introducing minimal distortions so was used for the majority of simulations.

The approach used to implement the 2-D and 1-D spectral filters is applicable to many other models. The 2-D convolution method can be implemented on any grid, though it suffers from being computationally expensive. The 1-D filter can be applied to irregular or more complex grids, but would require modification to separate the 2-D Gaussian function using an approximation that is appropriate for the particular grid.

Future work on spectral nudging in ACCESS will involve generalizing the spectral nudging to limited area and stretched grid configurations. Another potential approach to gaining a speedup in the convolution based spectral filter is to compute the convolutions over a small neighborhood, rather than the whole globe, ignoring areas where the Gaussian function has values close to zero. The ability to extend the convolution based spectral filter within the ACCESS/UM framework and in other modeling systems is an advantage of this approach.

~~Code availability~~

Code availability

Due to intellectual property right restrictions, CSIRO cannot publish the full source code for ACCESS or the UM. The Met Office Unified Model (UM) with the spectral nudging source code and configuration described in this paper can be obtained under an end user license

agreement (EULA) from CSIRO for educational and non-commercial research use for specific projects. To request a EULA for the modified UM, and/or to obtain the ACCESS1.3 model configuration used in this paper, please contact Tony Hirst (tony.hirst@csiro.au).

Acknowledgements. Thanks to Peter Dobrohotoff, John McGregor and Tony Hirst for their feedback in the preparation of the manuscript and the anonymous reviewers for suggested revisions to improve the manuscript. This research was undertaken with the assistance of resources from the National Computational Infrastructure (NCI), which is supported by the Australian Government. ~~The simulations were conducted on the raijin supercomputing cluster at the NCI (National Computing Infrastructure).~~ This work included funding by the Australian Government through the Australian Climate Change Science Programme. ERA-Interim data, from the European Centre for Medium-Range Weather Forecasts (ECMWF) was used in this research. The UM was made available to CSIRO under the Consortium Agreement: Met Office's Unified Model Earth System Modelling software (Met Office Ref L1587).

References

Bi, D., Dix, M., Marsland, S., O'Farrell, S., Rashid, H., Uotila, P., Hirst, A., Kowalczyk, E., Golebiewski, M., Sullivan, A., Yan, H., Hannah, N., Franklin, C., Sun, Z., Vohralik, P., Watterson, I., Zhou, X., Fiedler, R., Collier, M., Ma, Y., Noonan, J., Stevens, L., Uhe, P., Zhu, H., Griffies, S., Hill, R., Harris, C., and Puri, K.: The ACCESS coupled model: description, control climate and evaluation, Aust. Met. Oceanogr. J., 63, 41–64, 2013.

Davies, T., Cullen, M. J. P., Malcolm, A. J., Mawson, M. H., Staniforth, A., White, A. A., and Wood, N.: A new dynamical core for the Met Office's global and regional modelling of the atmosphere, Q. J. Roy. Meteor. Soc., 131, 1759–1782, doi:10.1256/qj.04.101, 2005.

Dee, D. P., Uppala, S. M., Simmons, A. J., Berrisford, P., Poli, P., Kobayashi, S., Andrae, U., Balmaseda, M. A., Balsamo, G., Bauer, P., Bechtold, P., Beljaars, A. C. M., van de Berg, L., Bidlot, J., Bormann, N., Delsol, C., Dragani, R., Fuentes, M., Geer, A. J., Haimberger, L., Healy, S. B., Hersbach, H., Hólm, E. V., Isaksen, L., Kållberg, P., Köhler, M., Matricardi, M., McNally, A. P., Monge-Sanz, B. M., Morcrette, J.-J., Park, B.-K., Peubey, C., de Rosnay, P., Tavolato, C., Thépaut, J.-N., and Vitart, F.: The ERA-Interim reanalysis: configuration and performance of the data assimilation system, Q. J. Roy. Meteor. Soc., 137, 553–597, doi:10.1002/qj.828, 2011.

Denis, B., Coté, J., and Laprise, R.: Spectral decomposition of two-dimensional atmospheric fields on limited-area domains using the discrete cosine transform (DCT), Mon. Weather Rev., 130, 1812–1829, 2002.

Dix, M., Vohralik, P., Bi, D., Rashid, H., Marsland, S., O'Farrell, S., Uotila, P., Hirst, T., Kowalczyk, E., Sullivan, A., Yan, H., Franklin, C., Sun, Z., Watterson, I., Collier, M., Noonan, J., Rotstayn, L., Stevens, L., Uhe, P., and Puri, K.: The ACCESS couple model: documentation of core CMIP5 simulations and initial results, Aust. Met. Oceanogr. J., 63, 83–99, 2013.

Jeuken, A., Siegmund, P., Heijboer, L., Feichter, J., and Bengtsson, L.: On the potential of assimilating meteorological analyses in a global climate model for the purpose of model validation, J. Geophys. Res.–Atmos., 101, 16 939–16 950, 1996.

Kanamaru, H. and Kanamitsu, M.: Scale-selective bias correction in a downscaling of global analysis using a regional model, Mon. Weather Rev., 135, 334–350, 2007.

Kida, H., Koide, T., Sasaki, H., and Chiba, M.: A new approach for coupling a limited area model to a GCM for regional climate simulations, J. Meteorol. Soc. Jpn., 69, 723–728, 1991.

Koffi, E. N., Rayner, P. J., Scholze, M., and Beer, C.: Atmospheric constraints on gross primary productivity and net ecosystem productivity: results from a carbon-cycle data assimilation system, Global Biogeochem. Cy., 26, 1–15, doi:10.1029/2010GB003900, 2012.

Kowalczyk, E., Stevens, L., Law, R., Dix, M., Wang, Y., Harman, I., Haynes, K., Srbinovsky, J., Pak, B., and Ziehn, T.: The land surface model component of ACCESS: description and impact on the simulated surface climatology, Aust. Met. Oceanogr. J., 63, 65–82, 2013.

Liu, P., Tsimpidi, A. P., Hu, Y., Stone, B., Russell, A. G., and Nenes, A.: Differences between downscaling with spectral and grid nudging using WRF, Atmos. Chem. Phys., 12, 3601–3610, doi:10.5194/acp-12-3601-2012, 2012.

Puri, K., Dietachmayer, G., Steinle, P., Dix, M., Rikus, L., Logan, L., Naughton, M., Tingwell, C., Xiao, Y., Barras, V., Bermous, I., Bowen, R., Deschamps, L., Franklin, C., Fraser, J., Glowacki, T., Harris, B., Lee, J., Le, T., Roff, G., Sulaiman, A., Sims, H., Sun, X., Sun, Z., Zhu, H., Chattopadhyay, M., and Engel, C.: Implementation of the initial ACCESS numerical weather prediction system, Aust. Met. Oceanogr. J., 63, 265–284, 2013.

Taylor, K., Stouffer, R. L., and Meehl, G. A.: An Overview of CMIP5 and the experiment design, B. Am. Meteorol. Soc., 93, 485–498, doi:10.1175/BAMS-D-11-00094.1, 2012.

Telford, P. J., Braesicke, P., Morgenstern, O., and Pyle, J. A.: Technical Note: Description and assessment of a nudged version of the new dynamics Unified Model, Atmos. Chem. Phys., 8, 1701–1712, doi:10.5194/acp-8-1701-2008, 2008.

Thatcher, M. and McGregor, J. L.: Using a scale-selective filter for dynamical downscaling with the conformal cubic atmospheric model, Mon. Weather Rev., 137, 1742–1752, doi:10.1175/2008MWR2599.1, 2009.

The HadGEM2 Development Team: G. M. Martin, Bellouin, N., Collins, W. J., Culverwell, I. D., Halloran, P. R., Hardiman, S. C., Hinton, T. J., Jones, C. D., McDonald, R. E., McLaren, A. J., O'Connor, F. M., Roberts, M. J., Rodriguez, J. M., Woodward, S., Best, M. J., Brooks, M. E., Brown, A. R., Butchart, N., Dearden, C., Derbyshire, S. H., Dharssi, I., Doutriaux-Boucher, M., Edwards, J. M., Falloon, P. D., Gedney, N., Gray, L. J., Hewitt, H. T., Hobson, M., Huddleston, M. R., Hughes, J., Ineson, S., Ingram, W. J., James, P. M., Johns, T. C., Johnson, C. E., Jones, A., Jones, C. P., Joshi, M. M., Keen, A. B., Liddicoat, S., Lock, A. P., Maidens, A. V., Manners, J. C., Milton, S. F., Rae, J. G. L., Ridley, J. K., Sellar, A., Senior, C. A., Totterdell, I. J., Verhoef, A., Vidale, P. L., and Wiltshire, A.: The HadGEM2 family of Met Office Unified Model climate configurations, Geosci. Model Dev., 4, 723–757, doi:10.5194/gmd-4-723-2011, 2011.

von Storch, H., Langenberg, H., and Feser, F.: A spectral nudging technique for dynamical downscaling purposes, Mon. Weather Rev., 128, 3664–3673, 2000.

Waldron, K., Paegle, J., and Horel, J.: Sensitivity of a spectrally filtered and nudged limited-area model to outer model options, Mon. Weather Rev., 124, 529–547, 1996.

Wang, Y., Leung, L. R., McGregor, J. L., Lee, D.-K., Wang, W.-C., Ding, Y., and Kimura, F.: Regional climate modelling: progress, challenges and prospects, J. Meteorol. Soc. Jpn., 82, 1599–1628, 2004.

Zhang, K., Wan, H., Liu, X., Ghan, S. J., Kooperman, G. J., Ma, P.-L., Rasch, P. J., Neubauer, D., and Lohmann, U.: Technical Note: On the use of nudging for aerosol–climate model intercomparison studies, Atmos. Chem. Phys., 14, 8631–8645, doi:10.5194/acp-14-8631-2014, 2014.

Table 1. Comparison of RMSE and GAE in air temperature ~~at 500~~measured in Kelvin, for one year of simulation excepting the first 10 days, using different nudging methods. Spectral nudging experiments use nudging applied once an hour. ~~Uncertainty quoted for GAE is based on a 95confidence interval~~

Experiment	RMSE			GAE		
	250 hPa	500 hPa	850 hPa	250 hPa	500
Control	4.25	4.69	5.08	-0.37	0.
Relaxation, soft	0.42	0.38	1.37	0.030	0.0
Relaxation, hard	0.32	0.26	1.39	0.15	0.0
Spectral, soft, $\lambda = 0.1$	~~0.03 ± 0.02~~ 0.68	0.64	1.55	-0.026	-0.
Spectral, ~~soft,~~ hard, $\lambda = 0.03$	0.35	0.29	1.37	0.13	0.0
Spectral, hard, $\lambda = 0.1$	~~0.65~~ 0.45	~~−0.05 ± 0.03~~ 0.41	1.36	0.081	-0.
~~Relaxation,~~ Spectral, hard, $\lambda = 0.2$	0.90	0.83	1.62	0.063	-0.

Table 2. Comparison of RMSE and GAE in U measured in m/s, for one year of simulation excepting the first 10 days, using different nudging methods. Spectral nudging experiments use nudging applied once an hour.

Experiment	RMSE			GAE		
	250 hPa	500 hPa	850 hPa	250 hPa	500 hPa	850 hPa
Control	18.26	3.09	8.25	0.70	0.21	-0.42
Relaxation, soft	1.32	1.00	1.35	-0.044	0.012	-0.12
Relaxation, hard	~~0.26~~ 0.77	~~0.07 ± 0.01~~ 0.58	0.97	-0.029	0.015	-0.068
Spectral, soft, $\lambda = 0.1$	2.67	2.28	2.28	-0.060	0.013	-0.12
Spectral, hard, $\lambda = 0.03$	1.01	0.78	1.12	-0.027	0.014	-0.068
Spectral, hard, $\lambda = 0.1$	1.74	1.54	1.76	-0.028	0.009	-0.072
Spectral, hard, $\lambda = 0.2$	3.59	3.09	2.71	-0.030	0.008	-0.072

Table 3. Comparison of RMSE and GAE in V measured in m/s, for one year of simulation excepting the first 10 days, using different nudging methods. Spectral nudging experiments use nudging applied once an hour.

Experiment	RMSE			GAE		
	250 hPa	500 hPa	850 hPa	250 hPa	500 hPa	850 hPa
Control	18.0	11.7	7.84	-0.061	0.021	-0.034
Relaxation, soft	1.47	1.09	1.34	0.006	0.020	0.003
Relaxation, hard	0.92	0.70	1.00	0.006	0.011	0.004
Spectral, soft, $\lambda = 0.1$	2.63	2.21	2.16	0.006	0.022	0.001
Spectral, hard, $\lambda = 0.03$	0.29 1.16	0.05 ± 0.01 0.91	1.14	0.007	0.013	0.007
Spectral, hard, $\lambda = 0.1$	0.41 1.72	-0.002 ± 0.02 1.47	1.65	0.007	0.014	0.012
Spectral, hard, $\lambda = 0.2$	0.83 3.47	-0.02 ± 0.05 2.96	2.57	0.006	0.016	0.011

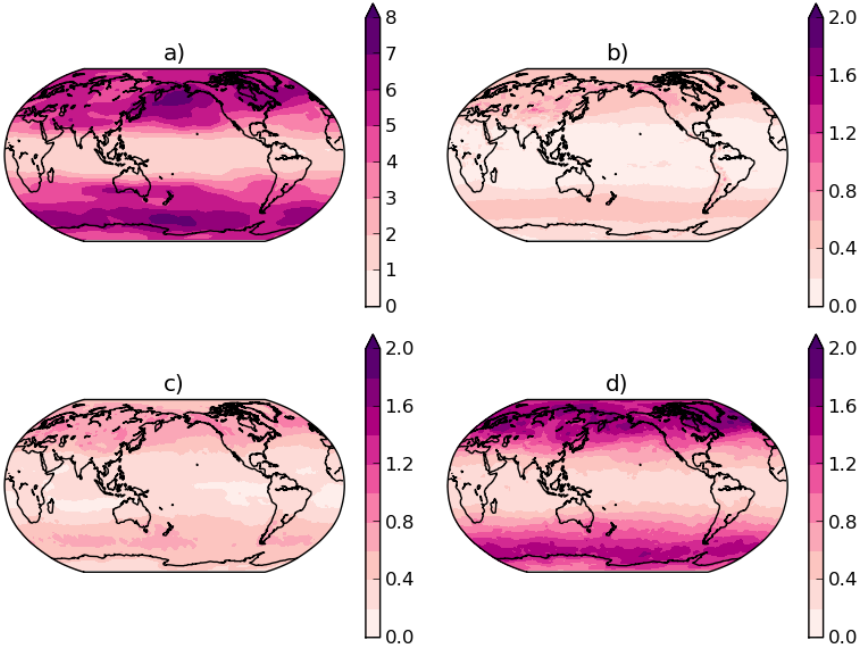

Figure 1. Spatial distributions of the RMSE in air temperature of ACCESS simulations. This is measured in Kelvin on a 2-D horizontal plane at 250 hPa and averaged over one year of simulation apart from the first 10 days. **(a)** is the control with no nudging. **(b)** is the relaxation nudging with hard nudging. **(c** and **d)** are spectral nudging using the 1-D filter with hard nudging, applied once an hour. Different nudging length scales were used: $\lambda = 0.1$ in **(c)** and $\lambda = 0.2$ in **(d)**. Note, for clarity, **(a)** uses a different scale for the contours.

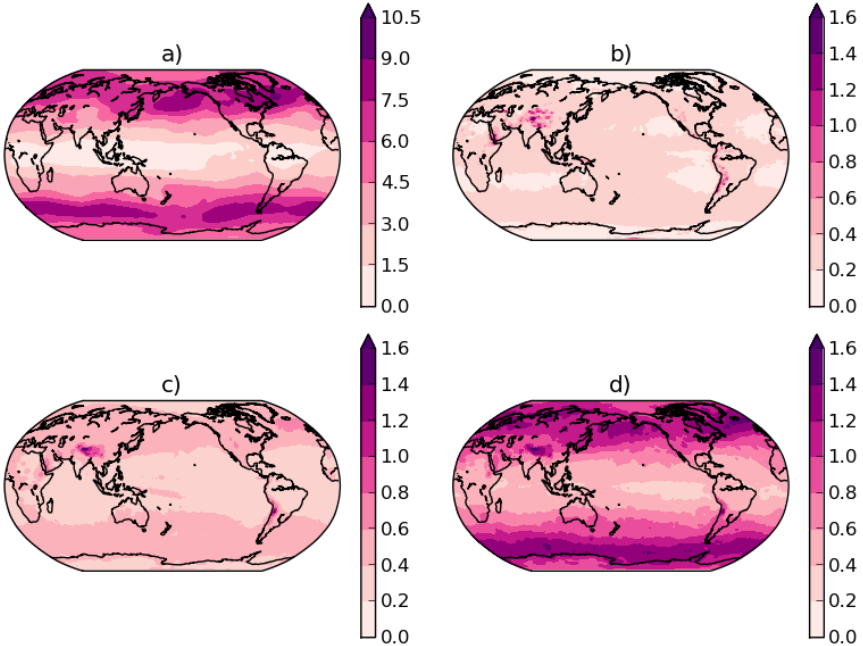

Figure 2. Spatial distributions of the RMSE in air temperature of ACCESS simulations. This is measured in Kelvin on a 2-D horizontal plane at 500 hPa and averaged over one year of simulation apart from the first 10 days. **(a)** is the control with no nudging. **(b)** is the relaxation nudging with hard nudging. **(c** and **d)** are spectral nudging using the 1-D filter with hard nudging, applied once an hour. Different nudging length scales were used: $\lambda = 0.1$ in **(c)** and $\lambda = 0.2$ in **(d)**. Note, for clarity, **(a)** uses a different scale for the contours.

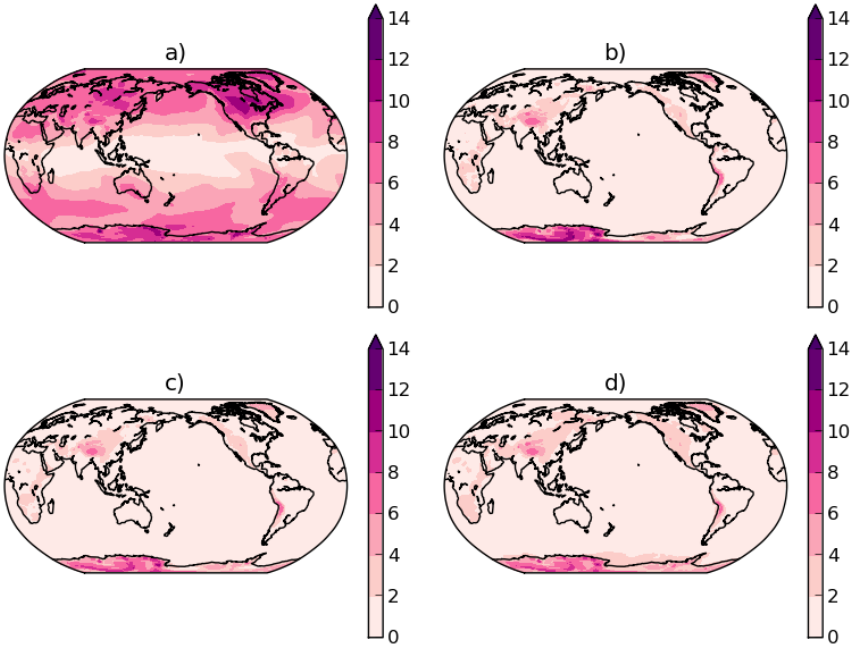

Figure 3. Spatial distributions of the RMSE in air temperature of ACCESS simulations. This is measured in Kelvin on a 2-D horizontal plane at 850 hPa and averaged over one year of simulation apart from the first 10 days. **(a)** is the control with no nudging. **(b)** is the relaxation nudging with hard nudging. **(c** and **d)** are spectral nudging using the 1-D filter with hard nudging, applied once an hour. Different nudging length scales were used: $\lambda = 0.1$ in **(c)** and $\lambda = 0.2$ in **(d)**.

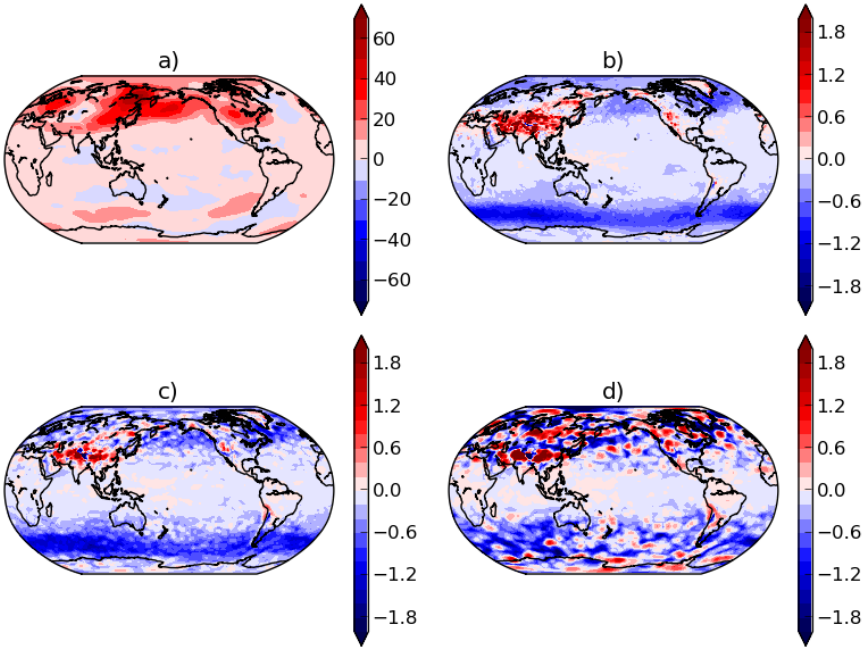

Figure 4. Spatial distributions of the ~~RMSE~~ difference in variance of air temperature ~~of~~ between ACCESS simulations and ERAI. This is measured in Kelvin squared, on a 2-D horizontal plane at 500 hPa and averaged over one year of simulation apart from the first 10 days. **(a)** is the control with no nudging. **(b)** is the relaxation nudging ~~with~~ hard nudging. **(c** and **d)** are spectral nudging using the 1-D filter with hard nudging, applied once an hour. Different nudging length scales were used: $\lambda = 0.1$ in **(c)** and $\lambda = 0.2$ in **(d)**. Note, for clarity, **(a)** ~~-~~uses a different scale for the contours.

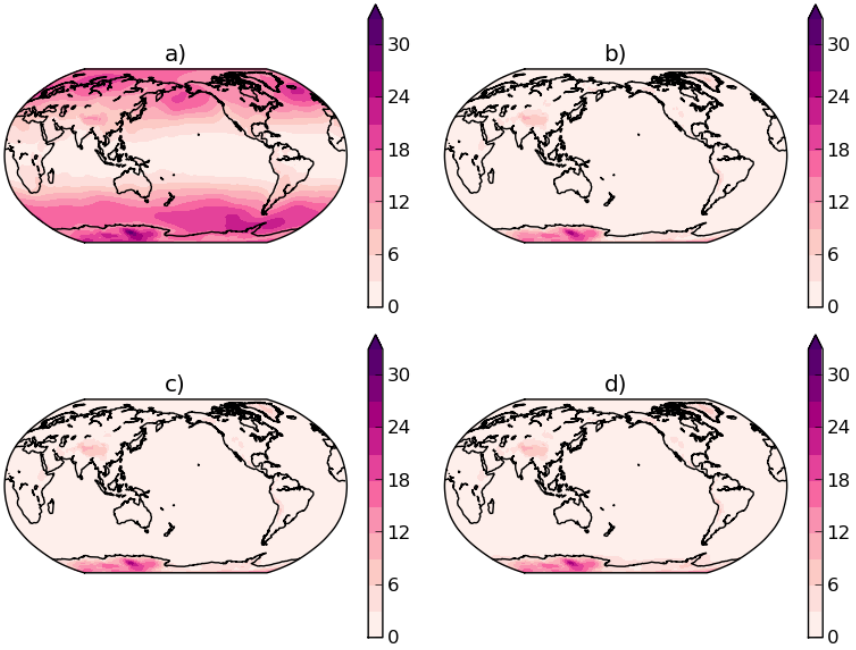

Figure 5. Spatial distributions of the ~~difference~~ RMSE for MSLP in ~~variance of air temperature~~ hPa, between ACCESS simulations and ERAI. This is ~~measured in Kelvin on a 2-D horizontal plane at 500and~~ averaged over daily mean values for one year of simulation apart from the first 10 days. **(a)** is the control with no nudging. **(b)** is the relaxation nudging hard nudging. **(c** and **d)** are spectral nudging using the 1-D filter with hard nudging, applied once an hour. Different nudging length scales were used: $\lambda = 0.1$ in **(c)** and $\lambda = 0.2$ in **(d)**. ~~Note, for clarity, (a) uses a different scale for the contours.~~

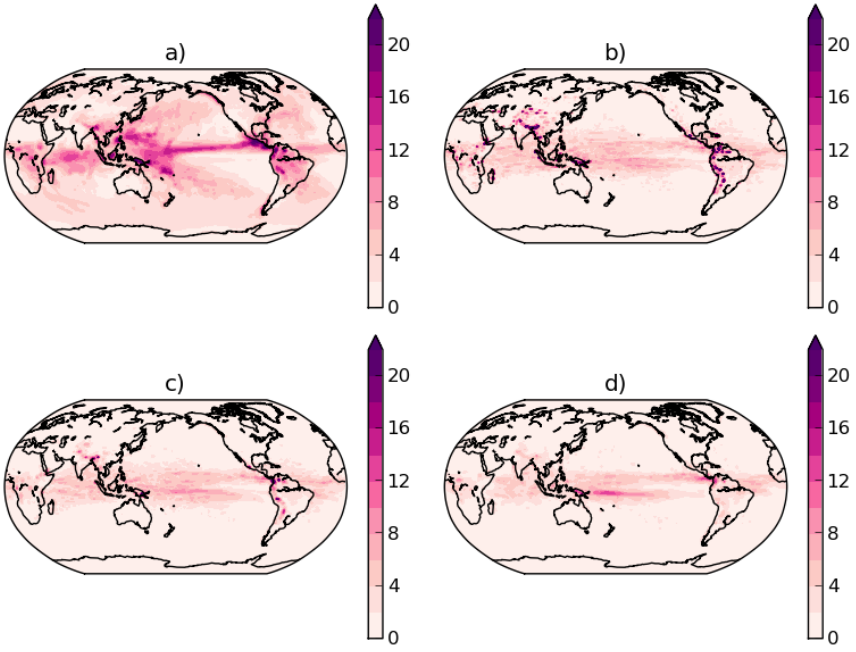

Figure 6. ~~RMS difference, in air temperature at 500,~~ Spatial distributions of ~~1-D filters compared to~~ the ~~2-D filter~~RMSE of montly mean precipitation in mm/day, between ACCESS simulations and ERAI. ~~Data was~~ This is averaged ~~temporally and zonally, for~~ over one year of ~~data sampled every time-step. Each~~ simulation~~uses~~ . **(a)** is the ~~same nudging parameters,~~ control with no nudging. **(b)** is the relaxation nudging hard nudging~~,~~. **(c** and **d)** are spectral nudging using ~~a~~ the 1-D filter ~~length scale of $\lambda = 0.1$~~with hard nudging, applied once an hour. Different nudging length scales were used: $\lambda = 0.1$ in **(c)** and $\lambda = 0.2$ in **(d)**.

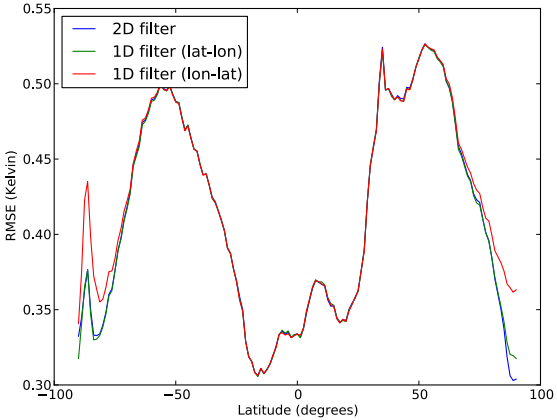

Figure 7. RMSE of air temperature at 500 hPa, of 1-D filters and 2-D filter compared to ERAI. Data was averaged temporally and zonally, for one year (apart from the first 10 days) of data sampled every six hours. Each simulation uses the same nudging parameters, with hard nudging, using a filter length scale of $\lambda = 0.1$, applied once an hour.

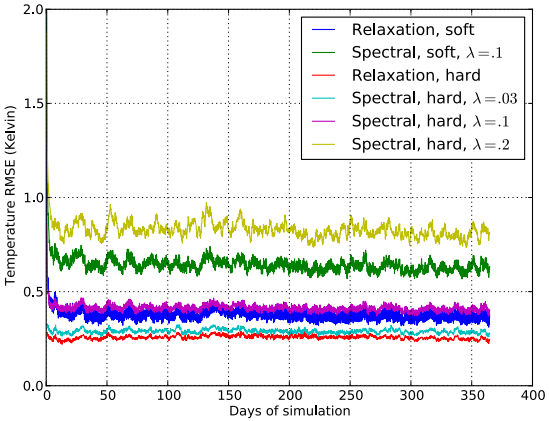

Figure 8. RMSE of temperature at 500 hPa, for a year of simulation. Simulations of relaxation and spectral nudging are compared, with strong or weak nudging, and several different spectral filter length scales. All of the spectral nudging simulations use the 1-D filter nudged once an hour.

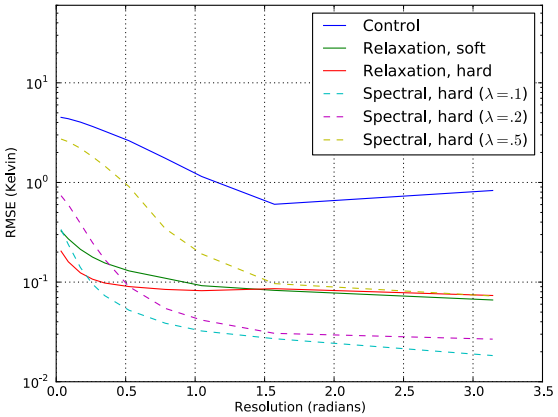

Figure 9. Plot of average RMSE of temperature at 500 hPa, at different regridded resolutions, for various simulations using nudging and a control simulation without nudging. All of the spectral nudging simulations use the 1-D filter nudged once an hour.

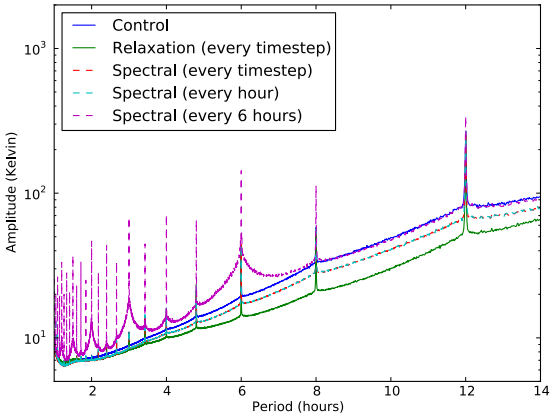

Figure 10. Temporal Fourier spectra for temperature at 500 hPa, for simulations with different nudging period. Soft nudging was applied and the spectral nudging simulations used a filter length scale of $\lambda = 0.1$.